Relative Stress Corrosion Susceptibilities of Alloys 690 and 600 in Simulated Boiling Water Reactor Environments

R. A. PAGE and A. McMINN

The relative susceptibilities of alloys 600 and 690 to intergranular stress corrosion cracking (IGSCC) in pure water and a simulated resin intrusion environment at 288 °C were evaluated. A combination of creviced and noncreviced slow-strain-rate, and precracked fracture mechanics tests were employed in the evaluation. Susceptibility was determined as a function of dissolved oxygen content, degree of sensitization, and crevice condition. The results indicated that alloy 600 was susceptible to various degrees of IGSCC in oxygen containing pure water when creviced, and immune to IGSCC when uncreviced. Alloy 690 was immune to IGSCC under all pure water conditions examined. Alloy 600 and alloy 690 were both susceptible to cracking in the simulated resin intrusion environment. Alloy 690, however, exhibited the greatest resistance to SCC of the two alloys.

I. INTRODUCTION

THE intergranular stress corrosion cracking (IGSCC) failure of an INCONEL* alloy 600 safe-end forging from the recirculation inlet nozzle of a boiling water reactor (BWR) in 1978 raised serious questions about the long-term suitability of alloy 600 for use in BWR environments. The results of a failure analysis on the safe-end indicated that the failure was caused by IGSCC occurring under the combined influence of high stresses and environmental conditions associated with a tight crevice between the safe-end and a thermal sleeve welded to the safe-end.[1] The cracking initiated in a weld heat affected zone and propagated through the weld made with INCONEL Welding Electrode 182 raising questions about its susceptibility and that of welds made with the similar INCONEL Filler Metal 82.

*A trademark of the INCO family of companies.

This failure indicated a need for further information concerning the IGSCC susceptibility of alloy 600, I-82, and I-182 under BWR operating conditions and a possible need for materials to replace them in BWR applications. A proposed replacement material for alloy 600 is the high chromium INCONEL alloy 690 which has thermal and mechanical properties similar to those of alloy 600 and which appears (based on limited test data) to be more resistant than alloy 600 to IGSCC. INCO has also developed high chromium weld alloys, R-127 and R-135, which are compatible with alloy 690 and could be used to replace I-182 and/or I-82.

This paper describes the results of a research program which was conducted to evaluate the IGSCC behavior of alloys 600 and 690 under conditions simulating present operating BWRs. The emphasis of the program was the determination of the relative IGSCC susceptibilities of alloys 600 and 690 and a better definition of the conditions under which the alloys may be susceptible to IGSCC. Results of similar tests on various weld metals are reported elsewhere.[2,3,4] Slow-strain-rate (SSR) tests were used to evaluate the effects of dissolved oxygen content, degree of sensitization, and crevice condition on the IGSCC susceptibility of both alloy 600 and 690 specimens. Crack-growth tests were conducted concurrently with the SSR tests to obtain data regarding the effects of stress intensity on crack propagation.

The primary coolant in a BWR is typically neutral pH, high purity water containing no additives, with radiolysis in the reactor core leading to an oxygen concentration of approximately 200 ppb. Tests were therefore conducted in a high purity water environment to simulate the "normal" primary coolant chemistry. However, water chemistry transients brought about by resin releases from the demineralizer system do occasionally introduce impurities into the primary coolant system. Since demineralizer resins rapidly decompose at normal operating temperatures to yield H_2SO_4, a lowered pH and an increased conductivity in the primary coolant system results. Thus, tests were also conducted in a simulated resin intrusion environment, which consisted of high purity water dosed with 1 ppm H_2SO_4. All tests were conducted at 288 °C.

II. EXPERIMENTAL

A single heat of alloy 600 and three heats of alloy 690 were studied. The alloy 600 was in the form of a 2.54 cm by 7.62 cm bar. The first heat of alloy 690 was in the form of 1.91 cm diameter rods, and the second and third heats were in the form of 2.54 cm thick plates. The chemical compositions of these alloys are listed in Table I. Room temperature and 288 °C tensile properties of the alloy 600 and the first heat of alloy 690 are listed in Table II.

Metallurgical conditions evaluated were selected to encompass the full range which exists in BWR environments, *i.e.*, as-received (AR), low temperature sensitized (LTS), furnace sensitized (FS), and a combination of furnace sensitized and low temperature sensitized. As-received signified material in the mill-annealed condition. Thermal treatments used were:

FS: 621 °C (1150 °F) for 24 hours
LTS: 449 °C (840 °F) for 24 hours

Sensitization treatments were performed on specimen blanks prior to machining. Modified Huey tests (48-hour exposure in boiling 25 pct nitric acid) were performed to

R. A. PAGE and A. McMINN are Senior Research Engineers, Southwest Research Institute, 6220 Culebra Road, P.O. Drawer 28510, San Antonio, TX 78284.

Manuscript submitted June 14, 1985.

Table I. Chemical Composition of Test Alloys

Element	Composition in Weight Percent			
	Alloy 600	Alloy 690[1]	Alloy 690[2]	Alloy 690[3]
Carbon	0.08	0.02	0.012	0.012
Nickel	72.82	60.62	59.86	60.02
Chromium	15.68	29.04	28.22	28.55
Iron	9.50	8.73	8.78	9.88
Manganese	0.21	0.31	0.32	0.25
Silicon	0.15	0.39	0.40	0.26
Copper	0.19	0.12	0.12	0.11
Aluminum	0.43	0.26	0.26	0.22
Titanium	0.16	0.40	0.39	0.27
Cobalt	0.02	0.03	0.02	0.05
Sulfur	0.007	0.006	0.005	0.006
Phosphorus	0.009	—	—	—

1 Heat #1 2 Heat #2 3 Heat #3

Table II. Tensile Properties of Alloys 600 and 690

	Alloy 600		Alloy 690 (Heat #1)	
	Room Temperature	288 °C	Room Temperature	288 °C
Yield strength, 0.2 pct offset, MPa	338	274	314	241
Ultimate tensile strength, MPa	739	679	702	622
Elongation, pct	35.9	40.4	44.9	47.2
Reduction in area, pct	56.9	53.3	67.6	66.5

determine the relative degree of grain boundary sensitization. As-received and heat-treated samples of alloys 600 and 690 were examined with conventional light microscopy (8:1 phosphoric acid electrolytic etch) and transmission electron microscopy (two-stage replicas of mechanically polished samples etched with glyceregia) in order to characterize the effect of various sensitizing treatments on carbide morphology.

The majority of the test matrix consisted of a series of slow-strain-rate (SSR) tests, with a lesser number of crack-growth tests also included. The SSR test provides an indication of SCC susceptibility in a relatively short time and is ideal for characterizing the effects of a number of variables since it accelerates crack initiation. The crack-growth tests were conducted concurrently with the SSR tests to obtain data regarding the effects of stress intensity on crack propagation.

The test loop used to conduct these tests is illustrated schematically in Figure 1. The loop incorporated three 3.8 liter autoclaves connected in parallel. To permit close control of oxygen content, all heated metallic portions of the loop were constructed of titanium alloys. For all the tests, the flow loop was operated in a recirculating mode with a flow rate of 11.4 1/h, *i.e.*, the fluid in each autoclave was replaced once each hour.

Solution chemistry was controlled by monitoring solutions entering and exiting the autoclaves and making adjustments, as required. Two 587 liter tanks were used to prepare and supply test fluids. Micropumps circulated fluid from the supply tanks and effluent from the autoclaves through the two monitoring loops. Solution conductivity, dissolved oxygen content, and pH of both the fluid from the supply tanks and the fluid leaving the autoclaves were monitored. The autoclaves were operated at 288 °C and 7.34 MPa.

Slow-strain-rate tests were performed in a six-specimen SSR system incorporated in one of the three autoclaves. This test facility, in which six specimens are tested in parallel, has been fully described elsewhere.[5] Each of the specimens was galvanically isolated from the autoclave, loading frame, load train, and other specimens by use of zirconia and Teflon inserts. Cylindrical, one-piece tensile specimens with cross-sectional diameters of 6.35 mm and gauge lengths of 25.4 mm were used. For each specimen the applied load and the potential *vs* a Ag/AgCl reference electrode of a design similar to that described by Magar and Morris[6] were monitored and recorded by a digital microcomputer. The crosshead displacement (related to the total strain experienced by each specimen) also was measured *via* a displacement transducer. Displacement was controlled by a screw-driven machine. A strain rate of 2×10^{-7} s^{-1} was used for all the SSR tests.

Crevices on the SSR specimens consisted of an inner layer of graphite cloth and an outer layer of nickel foil. Creviced specimens were exposed for 168 hours in the autoclave prior to the initiation of straining. This provided adequate time for the crevice chemistry to develop.[7] Straining of uncreviced specimens was initiated as soon as the autoclave temperature and oxygen level stabilized.

Crack-growth tests were conducted on 24.13 mm thick bolt-loaded wedge opening loading (WOL) specimens. Side grooves 1.21 mm deep were used to maintain a planar crack geometry and to increase the degree of constraint present at the surface and thus minimize the amount of crack tunneling. The WOL specimens were fatigue precracked in accordance with ASTM E 399 and bolt loaded to the desired stress intensity prior to exposure in the autoclave. Specimen potentials *vs* a Ag/AgCl reference electrode and a platinum wire were monitored throughout the test. The crack-growth

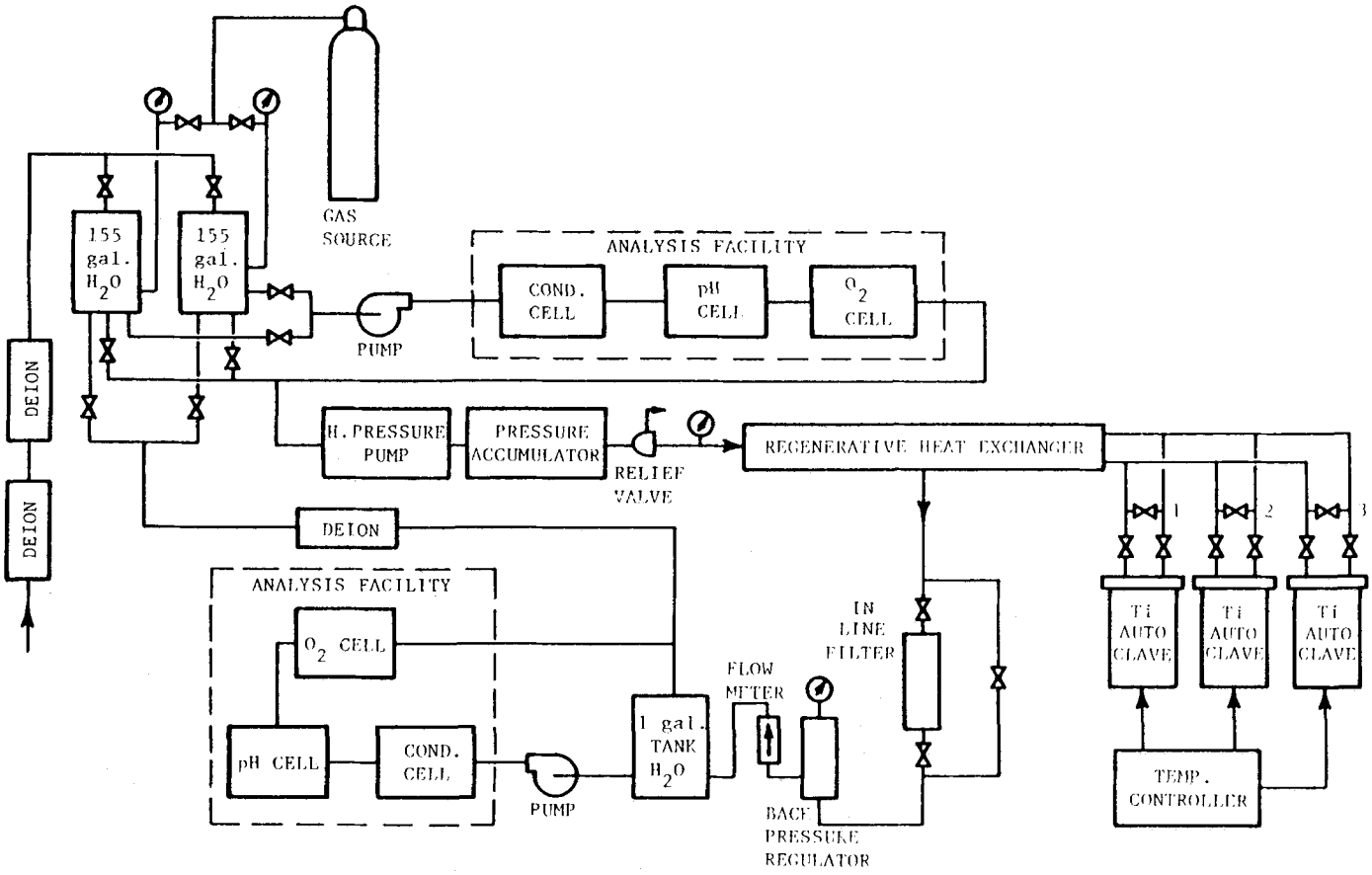

Fig. 1 — Schematic of BWR test loop.

specimens were removed and optically examined for crack growth once every 1000 to 1500 hours.

Tests were conducted in essentially two environments: a high purity water environment to simulate "normal" primary coolant chemistry, and a sulfuric acid dosed high purity water environment to simulate a resin intrusion environment. In the undosed high purity environment, creviced SSR specimens were run in water containing 16 ppm of dissolved oxygen to accelerate cracking. Uncreviced SSR specimens were run with either 8 ppm of dissolved oxygen to accelerate cracking or with 200 ppb of dissolved oxygen to simulate actual BWR levels. The conductivity of the influent water was always between 0.067 and 0.077 μS/cm. The conductivity of the effluent was approximately 0.2 μS/cm during the uncreviced SSR tests and approximately 1 μS/cm during the creviced tests. Influent and effluent oxygen levels differed by no more than 20 pct with the effluent level always slightly less than the influent level.

The simulated resin intrusion environment consisted of high purity water containing 1 ppm H_2SO_4. The addition of 1 ppm H_2SO_4 resulted in room temperature conductivity and pH of approximately 8 μS/cm and 4.8, respectively. All tests were run in an air saturated (~7 ppm dissolved oxygen) solution.

III. RESULTS

A. *Microstructure*

The three sensitizing heat treatments — low temperature sensitization, furnace sensitization, and a combination of furnace sensitization and low-temperature sensitization — did not produce a noticeable change in the microstructure of alloy 600. Figure 2 shows the microstructure of the alloy 600 in the AR, LTS, and FS conditions. The 8:1 phosphoric acid etch, which delineates grain boundaries in alloy 600 only if they are decorated with carbide precipitates, revealed numerous discrete carbide precipitates many of which appeared to outline grain boundaries. Continuous etching of the grain boundary did not occur, indicating that even the most severe sensitizing treatment employed did not produce a heavily sensitized microstructure. The TEM replicas confirmed the presence of discrete carbides and also indicated that many boundaries were relatively carbide free (Figure 3), and that some of the carbides that appeared to decorate grain boundaries in the optical micrographs were actually situated in the matrix (Figures 3(b) and 3(c)).

It was found that the 8:1 phosphoric acid etch delineated the grain boundaries in alloy 690, whether or not they were decorated by carbides. Thus, this etchant could not be used to discriminate sensitization for this alloy. The TEM replicas revealed that most of the grain boundary area in the alloy 690 specimens was free of carbides, whatever the heat treatment (Figure 4). This is consistent with the alloy's lower carbon content.

The microstructures suggest that a mild degree of sensitization may have been present in all of the alloy 600 specimens. Furthermore, the combination of the rather high carbon content and the minimal response to sensitization treatments indicates that very little of the carbon in the as-received alloy 600 was present in solid solution, *i.e.*, most of the carbon was present as precipitated carbides and thus

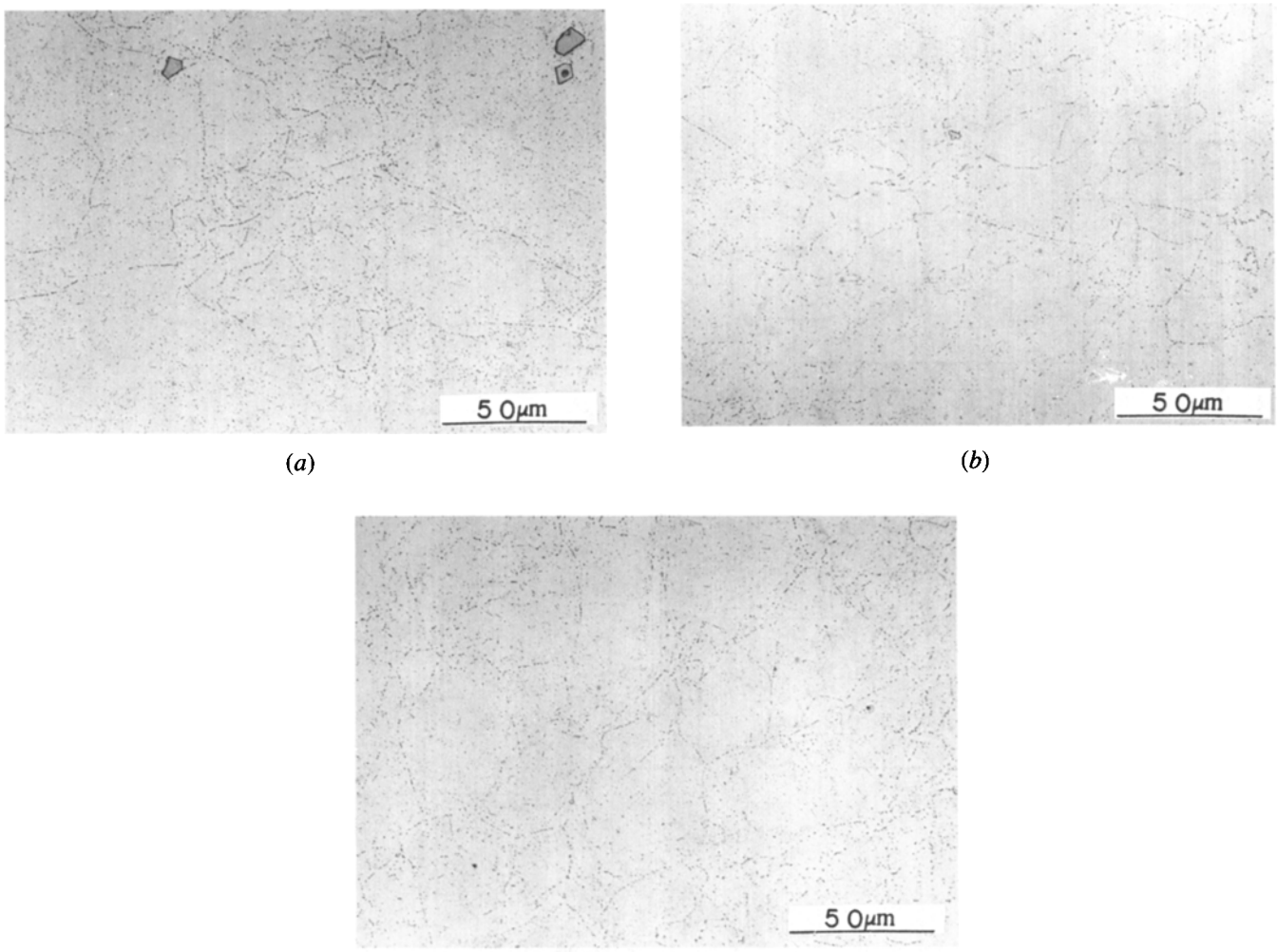

(*a*) (*b*) (*c*)

Fig. 2 — Microstructure of alloy 600 in (*a*) as-received, (*b*) low-temperature sensitized, and (*c*) furnace-sensitized condition.

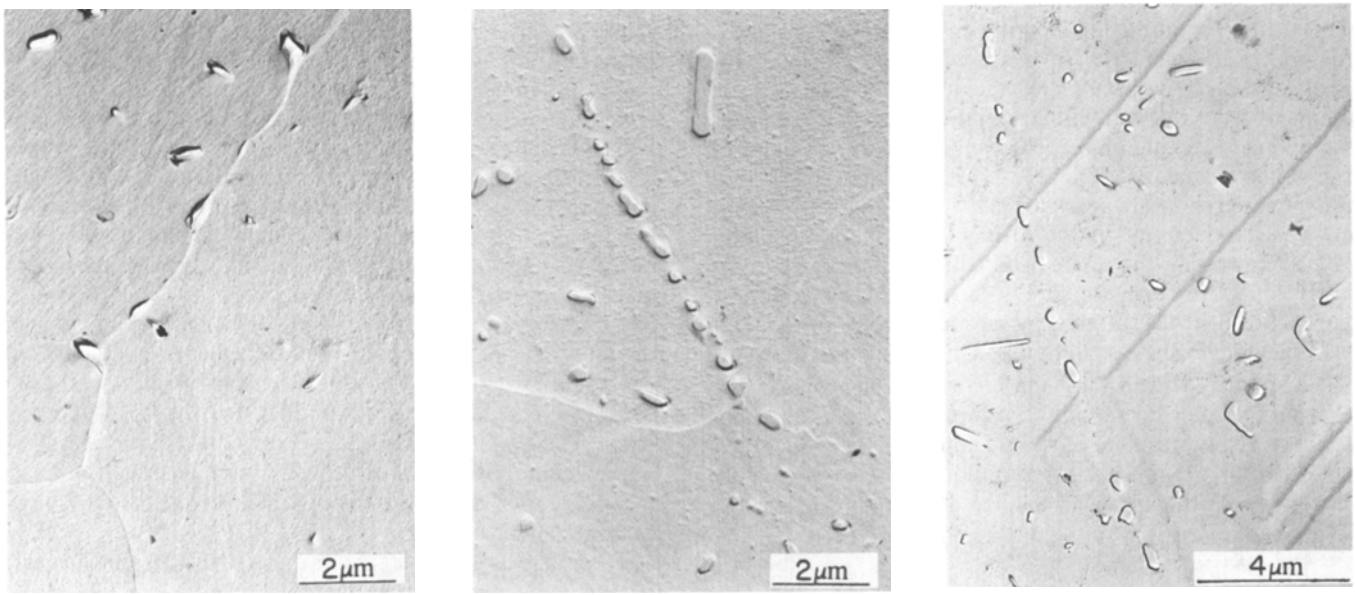

(*a*) (*b*) (*c*)

Fig. 3 — Carbide morphology of alloy 600 in (*a*) as-received, (*b*) low-temperature sensitized, and (*c*) furnace-sensitized condition.

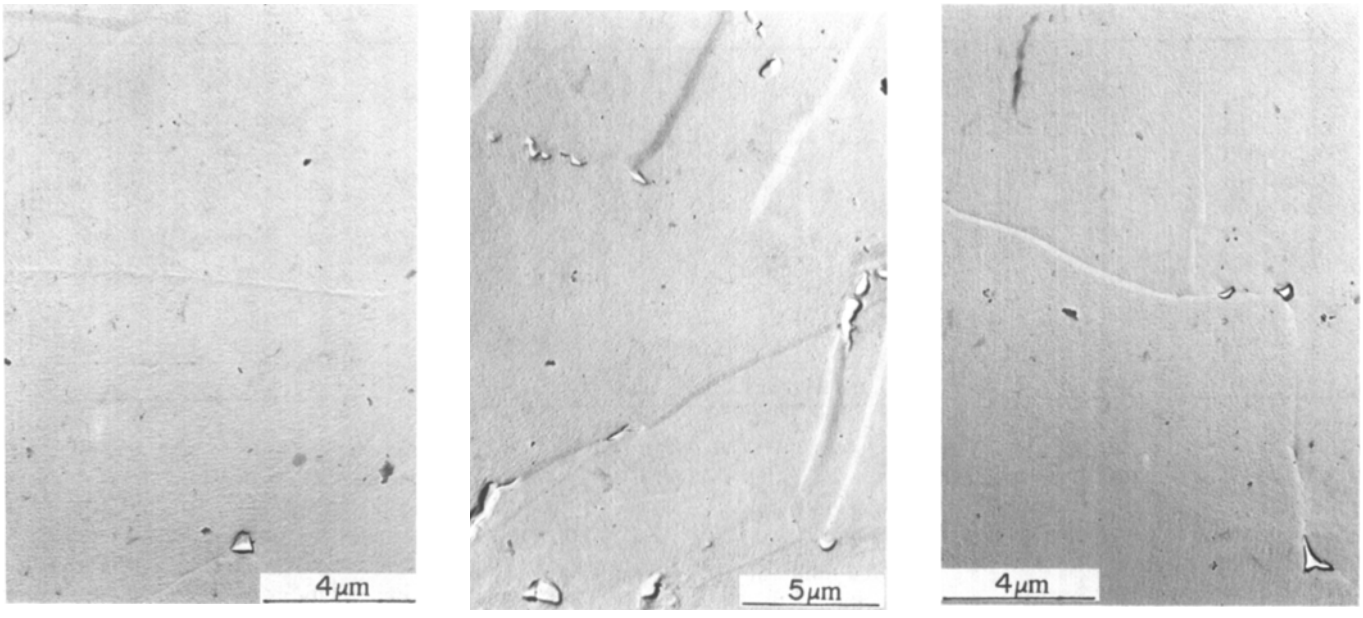

(*a*) (*b*) (*c*)

Fig. 4—Carbide morphology of alloy 690 heat 1 in (*a*) as-received, (*b*) low-temperature sensitized, and (*c*) furnace-sensitized condition.

unable to participate in sensitization. To determine the relative degree of grain boundary sensitization (caused by Cr depletion), modified Huey tests (48-hour exposure in boiling 25 pct nitric acid) were performed. The test results, presented in terms of weight loss and depth of penetration in Table III, indicate that the thermal treatments employed did not significantly alter the degree of sensitization of the as-received (AR) alloy 600, although the FS + LTS alloy 600 did corrode the most. A moderate weight loss, <1000 mg/dm^2/day compared to approximately 10,000 mg/dm^2/day for heavily sensitized alloy 600,[8] occurred independent of the particular thermal treatment. Alloy 690, on the other hand, was not susceptible to intergranular attack (negligible weight loss and no measurable penetration) in either the as-received or low-temperature sensitized condition.

Table III. Modified Huey Test Results

Material	Heat Treatment	Weight Loss Rate mg/dm^2/day	Penetration mm
alloy 600	AR[a]	212	0.18
alloy 600	LTS[b]	487	0.20
alloy 600	FS[c]	296	0.18
alloy 600	FS + LTS	694	0.48
alloy 690[1]	AR	2	0.00
alloy 690[1]	LTS	0	0.00

1 Heat #1
a As-received
b Low temperature sensitized—449 °C for 24 hours
c Furnace sensitized—621 °C for 24 hours

B. *High Purity Water*

Slow-strain-rate tests were conducted at 288 °C and a strain rate of 2×10^{-7} s^{-1} in high purity water containing 200 ppb or 8 ppm O_2 for uncreviced specimens and 16 ppm O_2 for creviced specimens. Complete data from all of the tests are tabulated in Tables IV and V. Included in the tables are test conditions, thermal treatment, mechanical properties measured during the test, specimen potential, time to failure, and an indication of whether or not SCC occurred. Both alloy 600 and alloy 690 demonstrated immunity to SCC in oxygen containing pure water in the uncreviced

Table IV. Test Data for Uncreviced Slow-Strain-Rate Tests in High Purity Water at 288 °C

Material	Heat Treatment	RA Pct	Elongation Pct	UTS MPa	Potential *vs* Ag/AgCl mV	Results	Time to Failure Hours	Oxygen Content ppm
alloy 600	AR[a]	49.9	35.6	579	−425	no SCC	490	0.2
alloy 600	LTS[b]	47.6	33.5	593	−480	no SCC	465	0.2
alloy 690[1]	AR	61.6	44.2	600	−410	no SCC	578	0.2
alloy 690[1]	LTS	47.6	41.3	621	−350	no SCC	584	0.2
alloy 600	AR	43.4	31.6	635	−190	no SCC	570	8
alloy 600	LTS	54.1	37.7	655	−210	no SCC	590	8
alloy 690[1]	AR	65.4	46.2	579	−230	no SCC	570	8
alloy 690[1]	LTS	55.9	45.6	648	−190	no SCC	700	8

1 Heat #1. a As-received. b Low temperature sensitized—449 °C for 24 hours.

Table V. Test Data for Creviced Slow-Strain-Rate Tests in High Purity Water at 288 °C and 16 ppm O_2

Material	Heat Treatment	RA Pct	Elongation Pct	UTS MPa	Potential *vs* Ag/AgCl mV	Results	Time to Failure Hours
alloy 600	AR[a]	61.7	40.7	662	−175	surface cracks	590
alloy 600	AR	50.4	32.9	821	−150	surface cracks	500
alloy 600	LTS[b]	49.9	40.6	724	−240	surface cracks	575
alloy 600	LTS	49.3	28.4	648	−165	surface cracks	565
alloy 690[1]	AR	67.0	53.7	586	−190	no SCC	660
alloy 690[1]	AR	66.6	50.6	538	−175	no SCC	690
alloy 690[1]	LTS	67.5	51.1	586	−160	no SCC	655
alloy 690[1]	LTS	69.3	49.1	600	−165	no SCC	685

1 Heat #1. a As-received. b Low temperature sensitized—449 °C for 24 hours.

condition. The fracture surfaces were entirely ductile in appearance; no surface cracking was observed. In the creviced condition, however, alloy 600 experienced shallow surface cracking, whereas alloy 690 demonstrated immunity to SCC. The mechanical properties of the specimens that did not show surface cracking were similar, but generally lower, to those produced in the 288 °C tensile tests. Differences in mechanical properties for these specimens are considered to be typical of material scatter.

The surface cracks in alloy 600 were found to be less than 100 μm deep, and the majority of the cracks were intergranular (Figure 5), although transgranular cracks were also observed (Figure 6). Surface cracking did not reduce the mechanical properties or the time to failure in the SSR tests. The shallow surface cracking indicates a borderline susceptibility to SCC.

Three WOL specimens were tested in the high purity water environment: alloy 600 welded with I-182 in the furnace sensitized and low-temperature sensitized condition, alloy 690 welded with I-182 in the low-temperature sensitized condition, and alloy 690 welded with I-182 in the furnace sensitized and low-temperature sensitized condition. The specimens were machined such that the cracks would propagate in the weld heat-affected zone, but for the alloy 600 specimen the cracking deviated into the base metal, and therefore the growth data generated were applicable to the base metal and not the weld metal.

The specimens were initially loaded to a stress intensity of 33 MPa · $m^{1/2}$, but no growth was detected after 1500 hours. At this point, the stress intensity was increased to 49 MPa · $m^{1/2}$ and the specimens were exposed for a further 6700 hours. Periodic examinations revealed a small amount of crack extension along the surface of the alloy 600 specimen, and no extension in either of the alloy 690 specimens.

The absence of SCC in the alloy 690 specimens was confirmed by examination of the fracture surfaces after the specimens had been broken open. However, the fracture surface of the alloy 600 specimen had 14.5 mm of stress corrosion crack growth (Figures 7 and 8). This corresponded to a final stress intensity of 31 MPa · $m^{1/2}$ and an average crack growth rate of 4.9×10^{-7} mm · s^{-1}.

For all the WOL specimens tested crack growth rates were determined by dividing the measured crack length by the time of the test. Since this procedure includes the time to initiate a stress corrosion crack from the fatigue precrack, actual crack growth rates will be greater than those calculated.

C. *Simulated Resin Environment*

Slow-strain-rate tests were conducted at 288 °C and a strain rate of 2×10^{-7} s^{-1} in the simulated resin intrusion environment. Complete data from all of the tests are tabulated in Table VI. Alloys 600 and 690 both exhibited

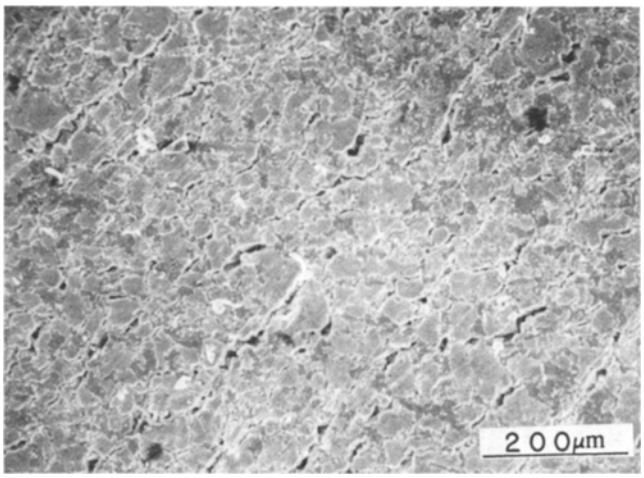

Fig. 5—Scanning electron micrograph of surface cracks in as-received alloy 600 SSR tested in a creviced condition at 288 °C in high purity water with 16 ppm O_2.

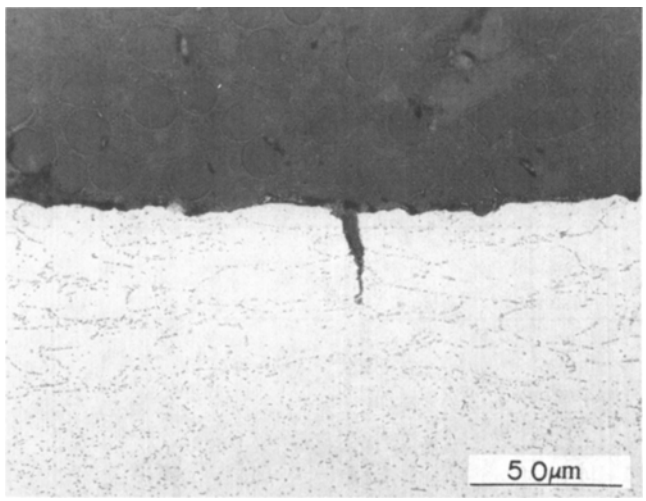

Fig. 6—Transgranular surface crack formed during SSR testing of creviced, low-temperature sensitized alloy 600 at 288 °C in high purity water with 16 ppm O_2.

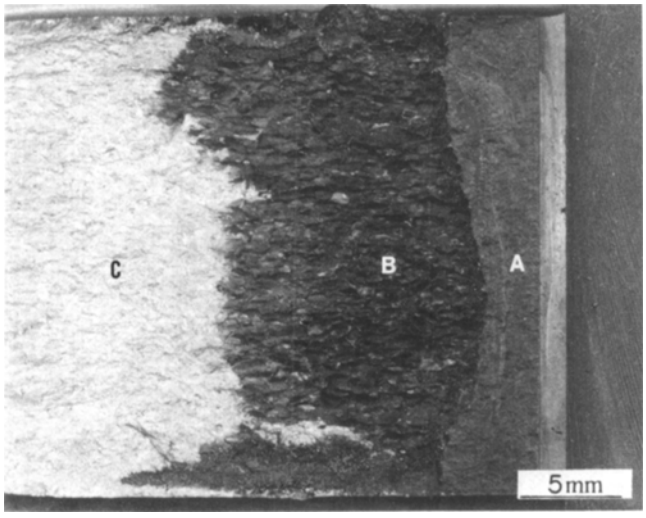

Fig. 7—Fracture surface of alloy 600/I-182 WOL specimen. Fatigue precrack (A), IGSCC (B), and room temperature air fracture (C) are shown.

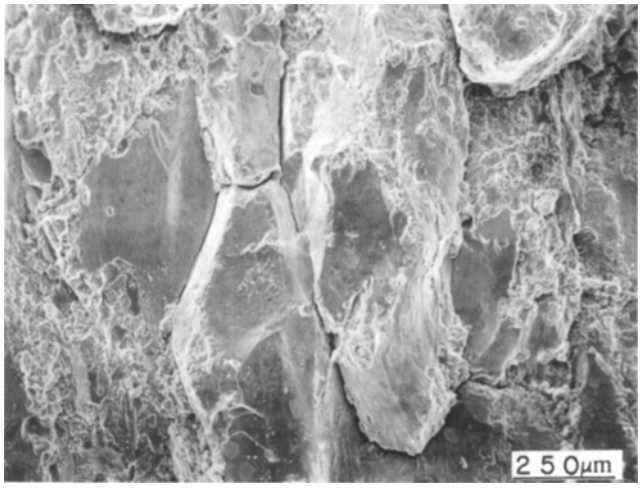

Fig. 8—Scanning electron micrograph of IGSCC through alloy 600, Location B, Fig. 7.

shallow surface cracking in the creviced and uncreviced condition, but otherwise the fracture surfaces were completely ductile. The surface cracking was generally less than 100 μm deep, intergranular, and did not affect the mechanical properties measured during the tests or the failure times. Figure 9 is typical of the extent of surface cracking observed. Some variability in response was observed since some specimens did not exhibit surface cracking. However, the variability was not dependent on heat treatment, material heat, or crevice conditions and therefore it is considered to be typical test-to-test variability often observed in SSR testing.

Four bolt-loaded WOL specimens were tested in the simulated resin intrusion environment. The alloys tested along with their heat treatments, initial stress intensities, and exposure times are listed in Table VII. As indicated in the table, the alloy 600 specimen was exposed for 4129 hours, whereas the three alloy 690 specimens were exposed for 3048 hours. The specimens were fractured at room tem-

Table VI. Slow-Strain-Rate Data for Resin Intrusion Environment at 288 °C

Material	Heat Treatment	RA Pct	Elongation Pct	UTS MPa	Potential *vs* Ag/AgCl mV	Results	Time to Failure Hours	Specimen Condition
alloy 600	AR[a]	21.6	39.0	727	+10	surface cracks	610	UC*
alloy 600	AR	27.6	36.4	723	−30	surface cracks	590	UC
alloy 600	LTS[b]	34.4	40.5	698	+40	surface cracks	600	UC
alloy 600	LTS	42.8	34.4	721	+20	surface cracks	575	UC
alloy 690[1]	AR	59.7	53.1	642	+40	surface cracks	745	UC
alloy 690[1]	AR	59.0	54.0	650	+40	surface cracks	710	UC
alloy 690[1]	LTS	67.3	56.8	658	+40	surface cracks	775	UC
alloy 690[1]	LTS	53.8	54.7	642	+50	surface cracks	750	UC
alloy 690[3]	AR	61.9	64.1	549	−50	no SCC	900	UC
alloy 690[3]	AR	64.2	62.2	565	−30	no SCC	880	UC
alloy 690[3]	LTS	67.1	59.5	562	−60	surface cracks	825	UC
alloy 690[3]	LTS	67.3	63.8	569	−30	no SCC	905	UC
alloy 690[3]	LTS	63.5	61.7	564	+ 5	no SCC	890	UC
alloy 600	AR	56.4	51.7	728	−10	no SCC	740	C[†]
alloy 600	AR	51.6	46.2	722	+ 5	no SCC	680	C
alloy 600	LTS	51.0	45.0	697	+40	surface cracks	660	C
alloy 600	LTS	47.0	42.1	697	−60	surface cracks	665	C
alloy 690[1]	AR	67.7	54.1	622	−10	surface cracks	780	C
alloy 690[1]	AR	64.0	52.6	635	− 5	surface cracks	740	C
alloy 690[1]	LTS	60.1	48.8	641	−10	surface cracks	700	C
alloy 690[1]	LTS	56.3	57.6	635	+30	surface cracks	860	C
alloy 690[3]	AR	68.6	63.1	566	−10	surface cracks	895	C
alloy 690[3]	AR	59.6	57.4	560	+30	surface cracks	880	C
alloy 690[3]	LTS	65.0	61.4	559	−10	surface cracks	895	C
alloy 690[3]	LTS	67.0	66.9	552	−50	surface cracks	915	C

1 Heat #1. 3 Heat #3.
a As-received. b Low temperature sensitized—449 °C for 24 hours.
* UC = uncreviced. † C = creviced.

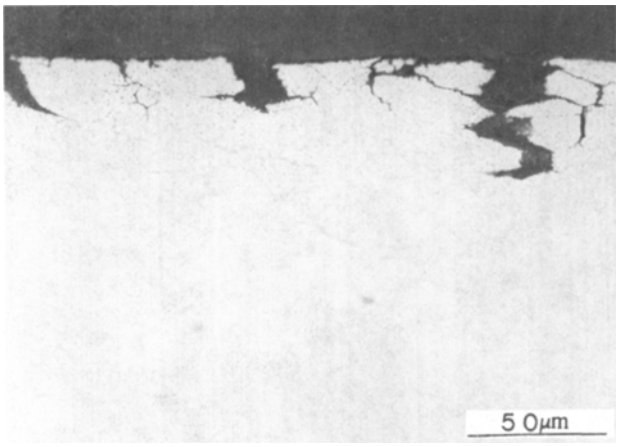

(*a*)

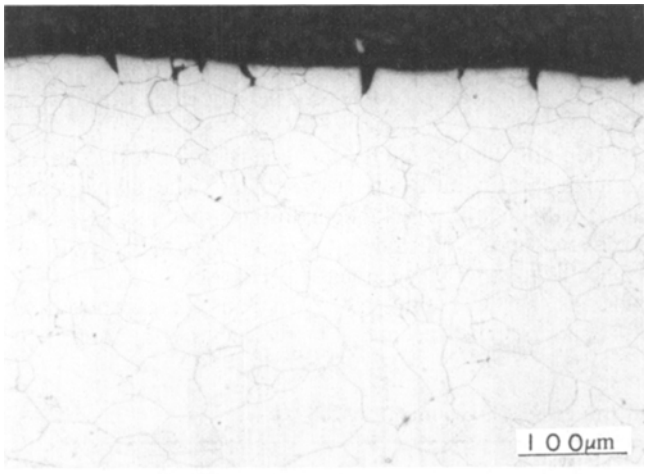

(*b*)

Fig. 9 — Typical surface cracking observed in (*a*) alloy 600 and (*b*) alloy 690 heat 1 during SSR testing in the simulated resin intrusion environment.

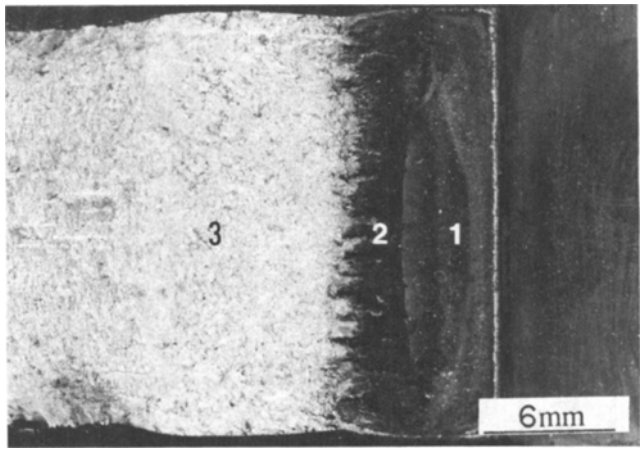

(*a*)

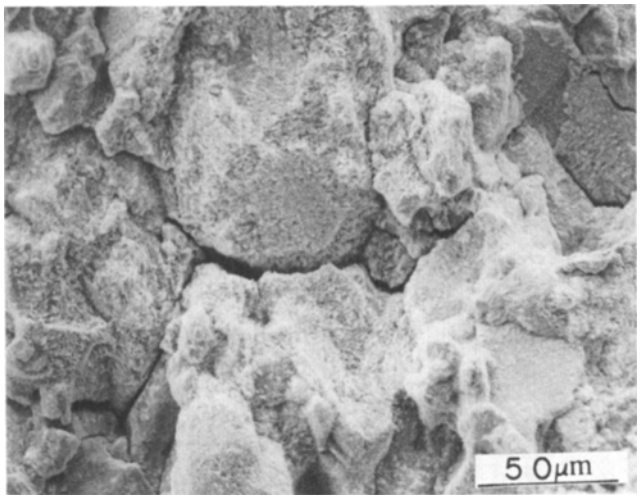

(*b*)

Fig. 10 — Fracture surface of alloy 600 WOL specimen. Fatigue precrack (1), IGSCC (2), and room temperature air fracture (3), are shown. Enlarged view of IGSCC is shown in (*b*).

perature following exposure so that the crack lengths could be accurately determined.

Examination of the alloy 600 fracture surface revealed the presence of IGSCC (Figure 10). The calculated crack growth rate was 3.2×10^{-7} mm · s^{-1}. Of the three alloy 690 specimens, only the specimen exposed at the highest initial stress intensity (70 MPa · $m^{1/2}$) experienced any crack growth. No evidence of SCC was observed on the specimens exposed with initial stress intensities of 50 and 60 MPa · $m^{1/2}$. Even at the relatively high stress intensity of 70 MPa · $m^{1/2}$, the observed crack growth rate of 2.2×10^{-8} mm · s^{-1} in alloy 690 was almost an order of magnitude less than that observed at a much lower stress intensity in alloy 600. The absence of cracking at 50 and 60 MPa · $m^{1/2}$ and the very slow growth rate observed at

Table VII. Crack Growth Data for Resin Intrusion Environment at 288 °C

Material	Heat Treatment	Exposure Time, Hours	Initial K, MPa · $m^{1/2}$	Crack Growth mm	Final K, MPa · $m^{1/2}$	Average Growth Rate, mm · s^{-1}
alloy 600	FS[a] + LTS[b]	4129	49.4	4.8	43.4[c]	3.2×10^{-7}
alloy 690[2]	FS + LTS	3048	50	0.0	45[d]	0.0
alloy 690[2]	FS + LTS	3048	60	0.0	54[d]	0.0
alloy 690[2]	FS + LTS	3048	70	0.24	63[d]	2.2×10^{-8}

2 Heat #2.
a Furnace sensitized — 621 °C for 24 hours.
b Low temperature sensitized — 449 °C for 24 hours.
c Reduction in K was due to a combination of crack growth and relaxation.
d Reduction in K was due entirely to load relaxation.

70 MPa · $m^{1/2}$ suggests that K_{ISCC} for alloy 690 in the simulated resin intrusion environment lies somewhere between 60 and 70 MPa · $m^{1/2}$. K_{ISCC} for alloy 600, on the other hand, is below 49 MPa · $m^{1/2}$. The fracture surface of the alloy 690 specimen that exhibited IGSCC is shown in Figure 11.

D. *Alloy Comparison*

The test results indicated that alloy 690 was more resistant to SCC than alloy 600 in both the oxygen containing pure water and the simulated resin intrusion environment. Crack-growth tests in oxygenated pure water produced crack growth rates in alloy 600 of 4.9×10^{-7} mm · s^{-1} for stress intensity in the range 49 to 31 MPa · $m^{1/2}$, whereas no growth was obtained for alloy 690 up to a stress intensity of 49 MPa · $m^{1/2}$. In the simulated resin intrusion environment, alloy 600 cracked at a rate of 3.2×10^{-7} mm · s^{-1} at a stress intensity of approximately 45 MPa · $m^{1/2}$, while alloy 690 experienced no crack growth at stress intensities of 60 MPa · $m^{1/2}$ and below and an average crack growth rate of 2.2×10^{-8} mm · s^{-1} at 70 MPa · $m^{1/2}$.

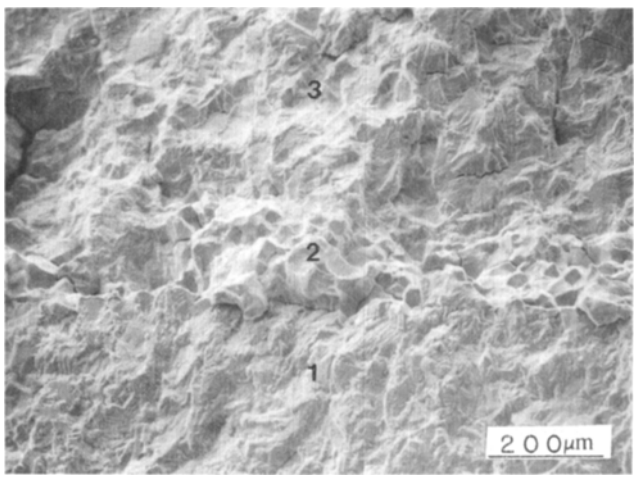

(*a*)

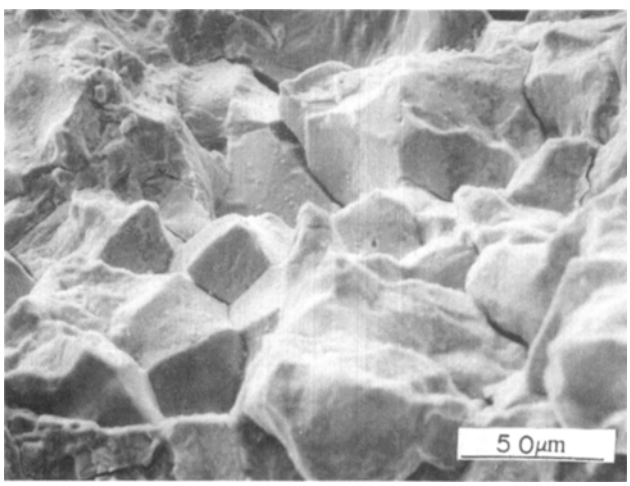

(*b*)

Fig. 11—Fracture surface of alloy 690 WOL specimen tested at 70 MPa · $m^{1/2}$. Fatigue precrack (1), IGSCC (2), and room temperature air fracture (3) are shown. Enlarged view of IGSCC is shown in (*b*).

In oxygenated pure water, SSR tests at 2×10^{-7} s^{-1} indicated borderline susceptibility (shallow surface cracks) for alloy 600 and immunity for alloy 690. In the simulated resin intrusion environment SSR tests, although both alloys 600 and 690 exhibited surface cracking, the cracks were more numerous and generally deeper in alloy 600.

Although alloy 690 did not demonstrate cracking susceptibility in any of the oxygenated pure water tests, it should not be concluded from these results that it is immune to SCC in oxygen containing pure water, only that it is more resistant than alloy 600. Immunity under more severe mechanical conditions, *i.e.*, higher stress intensity or lower strain rate, must still be demonstrated.

IV. DISCUSSION

Although BWRs operate at temperatures near 288 °C and oxygen levels of approximately 200 ppb, the more extensive use of alloy 600 in PWR components has stimulated research into the problem of stress corrosion cracking under conditions more representative of PWR service, *i.e.*, deaerated water at 315 to 345 °C or in caustic solutions which are believed to occur in crevices. Very little data have been generated under BWR conditions. A number of factors regarding the SCC susceptibility of alloy 600 are apparent from the literature, however. Hubner *et al.*[9] identified two potential regimes in which cracking occurred. The first regime is in the strongly cathodic region and probably corresponds to about −0.5 to −0.6 V_{SHE}. The second potential regime identified by Hubner *et al.* was just below the transpassive region at approximately 0.6 to 0.7 V_{SHE}. Vermilyea,[10,11] on the other hand, has identified cracking at 0.0 V_{SHE} and above but not at −0.2 and −0.4 V_{SHE} at pH 2.5. At oxygen levels approaching zero, the corrosion potential of alloy 600 at 288 °C is about −0.75 V_{SHE}, while at levels above 1 ppm the potential is at or above −0.10 V_{SHE}.[12] Thus the lower potential regime for IGSCC corresponds to a zero oxygen level and the upper regime for IGSCC, as identified by Vermilyea, corresponds to oxygen levels above about 1 ppm.

The slow-strain-rate results obtained for alloy 600 are consistent with the above observations. Immunity to IGSCC was observed with 200 ppb of oxygen present. The potentials of these tests, −0.37 to −0.24 V_{SHE}, (−0.48 to −0.35 Ag/AgCl) were in the range of immunity identified by Vermilyea and the range of immunity identified by Hubner *et al.* With an oxygen content of 8 ppm, cracking was not observed even though the potentials, −0.14 to −0.08 V_{SHE}, were near the regime where Vermilyea reported susceptibility at a pH of 2.5. These tests were uncreviced samples, however, and it has been suggested that crevices are necessary to crack alloy 600 in oxygen containing water.[13] Several workers have, however, reported failures of uncreviced specimens at oxygen levels above 400 ppb.[14,15,16] The slow-strain-rate results for creviced samples in water containing 16 ppm of oxygen showed borderline behavior, *i.e.*, the formation of shallow surface cracks, for alloy 600, but the crack-growth tests indicated IGSCC susceptibility for alloy 600. The fatigue precrack acts as a tight crevice; thus these results should be considered as creviced tests in oxygen containing water. The above results are consistent with van Rooyen's sugges-

tion[13] that crevices are necessary for IGSCC of alloy 600 in aerated water.

The present results indicate that alloy 690 is immune to IGSCC in oxygen containing water at 288 °C in both the creviced and the uncreviced conditions. The crack growth tests indicate that a stress intensity of 49 MPa · $m^{1/2}$ is insufficient for crack propagation. Hence, K_{ISCC} must be greater than 49 MPa · $m^{1/2}$. The slow-strain-rate tests, usually a very severe test for susceptibility, also were unable to initiate IGSCC in alloy 690. These results are all consistent with previous demonstrations of IGSCC immunity in pure water and chlorinated water tests[11,17,18] and with the findings that increasing chromium concentration improves IGSCC resistance in high-temperature pure water.[18] This behavior also is consistent with previous U-bend results which indicated a strong effect of chromium content on SCC of weld metals.[3] In those tests, welds containing less than 24 pct chromium cracked easily, while welds containing more than 24 pct chromium were significantly more resistant. Hence, it can be concluded that bulk chromium plays an important role in the SCC behavior of these nickel base alloys with higher chromium leading to increased resistance to SCC in typical BWR environments. This increased resistance could be due to a smaller chromium depleted zone or a more protective passive film or both.

Comparison of the results in the simulated resin intrusion environment with those obtained in pure water indicates that the addition of 1 ppm H_2SO_4 enhanced cracking. The amount of surface cracking in SSR tests of alloys 600 and 690 was increased by the addition of the sulfuric acid. The rate of crack growth in alloy 600 was not increased, however, with values of 4.9×10^{-7} mm · s^{-1} and 3.2×10^{-7} mm · s^{-1} obtained in pure water and water containing 1 ppm H_2SO_4, respectively. The acceleration of cracking through H_2SO_4 additions has also been demonstrated by Andresen,[19] for alloy 600, and by Floreen,[3] for a number of INCONEL weld metals.

Although the simulated resin intrusion environment provided a more severe test of SCC resistance than pure water, even more severe conditions may occur during service. The 1 ppm H_2SO_4 addition utilized in this program resulted in a room temperature conductivity of approximately 8 μS/cm. However, conductivity excursions to approximately 55 μS/cm have been observed.[19,20] Based on the results of Andresen,[19] the 55 μS/cm environment would be considerably more aggressive than the 8 μS/cm environment employed in this work. Additionally, in the presence of sulfuric acid, the 200 ppb oxygen level in BWRs appears to be more aggressive than the 7 ppm level employed in this program. Hence, the behavior observed in the simulated resin intrusion environment does not represent the worst case expected during service.

The heat of alloy 600 used in this study had an as-received microstructure typical of a high carbon heat which had been heat treated at a temperature low enough that carbides precipitated during prior manufacturing steps were not fully dissolved. In this condition much less carbon is expected to be in solution. The lack of sensitization achieved during LTS or FS treatments was consistent with the minimal amount of carbon remaining in solution. Thus one of the key factors in determining the effect of sensitization is the carbon content in solution. The lack of sensitization observed for the alloy 690 was also consistent with its lower carbon content. It was not surprising that there was no correlation observed between IGSCC and the heat-treated condition of the alloys. Other heats of these alloys with different thermal treatments and microstructures may not exhibit the same SCC susceptibility as the materials studied in this program, and this should be borne in mind when comparing the results presented here with those of other investigators.

V. CONCLUSIONS

The following conclusions can be drawn from the results obtained in the present investigation:

1. In an uncreviced geometry alloys 600 and 690 were immune to SCC at 288 °C in oxygen containing pure water.
2. In a creviced geometry alloy 600 was susceptible to IGSCC at 288 °C in oxygen containing pure water. Cracks propagated at a stress intensity of 31 MPa · $m^{1/2}$.
3. Alloy 690 was immune to SCC in pure water under all conditions evaluated. Fatigue precracks did not propagate at a stress intensity of 49 MPa · $m^{1/2}$.
4. The addition of 1 ppm H_2SO_4 to oxygen containing pure water resulted in increased cracking in alloy 600 and alloy 690. Hence, the increased acidity and conductivity associated with the addition produced a more severe environment in terms of SCC propensity.
5. Ranking of the alloys in terms of their SCC resistance in the simulated resin intrusion environment indicated that alloy 600 had a lower resistance than alloy 690. This ranking also correlates with the bulk chromium content suggesting that increased chromium concentration provides an increased resistance to SCC in BWR environments.
6. Alloy 690 was susceptible to SCC in the simulated resin intrusion environment. Cracks were found to propagate at a stress intensity of 70 MPa · $m^{1/2}$ but not at 50 or 60 MPa · $m^{1/2}$. This suggests that K_{ISCC} is between 60 and 70 MPa · $m^{1/2}$.

ACKNOWLEDGMENTS

This work was funded by the Electric Power Research Institute (EPRI) and was conducted as part of EPRI Research Project 1566-1. The authors would like to thank Drs. J. L. Nelson, W. J. Childs, and A. R. McIlree for their valuable discussions throughout the period of this program.

REFERENCES

1. H. C. Burghard and A. J. Bursle: Final Report, Project 02-5839-001. Southwest Research Institute, San Antonio, TX, December 1978.
2. R. A. Page: *Corrosion*, 1983, vol. 39, pp. 409-21.
3. S. Floreen: Sixth Semi-Annual Report, RP 1566-2, International Nickel Company, Suffern, NY, March-August 1982.
4. A. McMinn and R. A. Page: Proceedings of the Second International Symposium on Environmental Degradation of Materials in Nuclear Power Systems — Water Reactors, Monterey, CA, Sept. 9–12, 1985, in press.
5. F. F. Lyle, Jr. and E. B. Norris: *Stress Corrosion Cracking–The Slow Strain-Rate Technique*, ASTM STP 665, A. M. Ugiansky and J. H. Payer, eds., ASTM, Philadelphia, PA, 1979, pp. 388-98.
6. I. J. Magar and P. E. Morris: *Corrosion*, 1976, vol. 32, pp. 374-77.
7. D. F. Taylor: *Corrosion*, 1979, vol. 35, pp. 550-59.
8. G. P. Airey: EPRI Final Report NP-1354, Electric Power Research Institute, Palo Alto, CA, March 1980.
9. W. Hubner, M. Pourbaix, and G. Ostberg: *Proc. of 4th Int. Cong. on Met. Corrosion*, NACE, Houston, TX, 1972, pp. 65-74.

10. D. A. Vermilyea: *Corrosion*, 1975, vol. 31, pp. 421-24.
11. D. A. Vermilyea: *Corrosion*, 1973, vol. 29, pp. 442-48.
12. M. E. Indig and A. R. McIlree: Report No. NEDO-12709, General Electric, Pleasanton, CA, May 1978.
13. D. van Rooyen: *Corrosion*, 1975, vol. 31, pp. 327-37.
14. H. Coriou, L. Grall, P. Olivier, and H. Willermoz: *Fundamental Aspects of Stress-Corrosion Cracking*, NACE, Houston, TX, 1969, pp. 352-59.
15. W. Hubner, B. Johansson, and M. Pourbaix: A. G. Atomenergi Report AE-437, Studsvik, Nykoping, Sweden, 1971.
16. B. Gronwall, L. Ljungberg, W. Hubner, and W. Stuart: *Nuclear Eng. and Design*, 1967, vol. 6, pp. 383-90.
17. H. R. Copson, D. van Rooyen, and A. R. McIlree: *Proceedings of the Fifth International Congress on Metallic Corrosion*, NACE, Houston, TX, 1974, pp. 376-79.
18. A. J. Sedricks, J. W. Schultz, and M. A. Cordovi: *Boshoku Gijutsu*, 1979, vol. 28, no. 2, pp. 82-95.
19. P. L. Andresen: Paper No. 177, Corrosion 84, NACE, Houston, TX, 1984.
20. B. Francis, F. M. Kustas, and E. C. Martin: Second Progress Report, EPRI RP 1563-2, Pacific Northwest Laboratories, Richland, WA, June 1980.